# Supercritical Fluid Fractionation of Copolymers Based on Chemical Composition and Molecular Weight

J. ALAN PRATT, SANG-HO LEE, and MARK A. McHUGH*

Department of Chemical Engineering, Johns Hopkins University, Baltimore, Maryland 21218

SYNOPSIS

Poly(ethylene-*co*-methyl acrylate) copolymers of 30, 40, 60, and 70 wt % acrylate in the backbone have been fractionated with supercritical (SCF) propane, propylene, butane, 1-butene, and chlorodifluoromethane. The fractionations were performed isothermally using an increasing pressure profile that provided gram-sized fractions with molecular weight distributions of ~ 1.2 to 2.2 as compared to those of the parent copolymers, which were ~ 2.6 to 3.5. If the chemical composition distribution of the copolymer is greater than ±2%, it is possible to fractionate with respect to chemical composition by chosing solvents that preferentially dissolve the nonpolar ethylene-rich or the polar acylate-rich oligomers. Cloud-point curves were determined for each copolymer in the SCF solvents to provide an indication of whether the solvent would dissolve the copolymer at temperatures and pressures within the range of the fractionation apparatus. © 1993 John Wiley & Sons, Inc.

## INTRODUCTION

Many of the principles that govern the fractionation of polymers with liquid solvents also are operative with supercritical fluid solvents except that with supercritical fluid (SCF) solvents there is the additional degree of freedom that the solvent power can be more finely tuned using pressure. Because of their variable solvent strengths, SCF solvents are ideal candidate solvents for fractionating polymers. From a process standpoint, the sharp decrease in polymer solubility with decreasing pressure makes SCF solvents amenable for process recycle and the rapid disengagement of the gaseous SCF solvent at low pressure promotes facile recovery of a solvent-free polymer. Recently, many reports have emerged describing the potential of using SCF solvents to fractionate and purify polymers with respect to molecular weight, chemical composition, and backbone structure.[1-14] An overview of the techniques and underlying principles involved with supercritical fractionation is presented by McHugh and Krukonis.[6]

Krukonis and co-workers[3,11] were the first to demonstrate that polymers could be fractionated by chemical composition as well as by molecular weight using SCF solvents. They fractionated styrenic–acrylic copolymers with supercritical hydrocarbons and found that they could obtain fractions of narrow molecular weight distribution and with differing composition. A general conclusion from their study was that, compared with liquid antisolvent fractionation, SCF fractionation is a more rapid technique that provides gram-sized samples of narrow molecular weight distribution.

Watkins et al.[11,12] showed that temperature rising elution fractionation, a technique developed for conventional liquid fractionation, could also be used for SCF fractionation. With this technique, it is possible to fractionate a semicrystalline polymer with respect to the number of short-chain branches along the backbone of the polymer. They control the solubility of the various oligomers by carefully melting oligomers of a fixed backbone structure. Once the oligomers melt, they quickly dissolve in the SCF solvent since the operating pressure is maintained at a high level where the liquefied oligomers are miscible with the SCF solvent, although the remaining semicrystalline, solid polymer is vir-

* To whom correspondence should be addressed.

Journal of Applied Polymer Science, Vol. 49, 953–966 (1993)
 CCC 0021-8995/93/060953-14

tually insoluble in the SCF solvent. The crystallization temperature of the oligomers is largely dependent on the backbone structure provided that the molecular weight of the chains is sufficiently high so that the chain ends of the polymers do not contribute significantly to the disruption of local order.

The choice of an appropriate SCF solvent and the operating conditions for a fractionation depends intimately on the location of the cloud-point curve in P–T space for the copolymer–SCF solvent system of interest. The location of the cloud-point curve depends on the intermolecular forces in operation between solvent–solvent, solvent–polymer segment, and polymer segment–segment pairs in solution and on the free-volume difference between the polymer and the solvent. It is instructive to consider how the intermolecular potential energy of an $i$–$j$ pair of segments or molecules, $\Gamma_{ij}$, depends on the physical properties of the polymer–solvent pair using the following simplified expression provided by Prausnitz et al.[15]:

$$\Gamma_{ij} \approx -C_1 \frac{\alpha_i \alpha_j}{r^6} - C_2 \frac{\mu_i^2 \mu_j^2}{r^6 kT} - C_3 \frac{Q_i^2 Q_j^2}{r^{10} kT} - C_4 \frac{\mu_i^2 Q_j^2}{r^8 kT} - C_5 \frac{\mu_j^2 Q_i^2}{r^8 kT} + \text{Hydrogen bonding} \quad (1)$$

where the first term on the right-hand side, written in terms of the polarizabilities, $\alpha_i$, represents dispersion interactions; the second term, written in terms of the dipole moments, $\mu_i$, represents dipolar interactions; the third, fourth, and fifth terms, written in terms of the quadrupole moments, $Q_i$, represent quadrupolar interactions; and the final term, written symbolically, represents hydrogen-bonding interactions. In this equation, $r$ is the distance between the molecules; $k$, Boltzmann's constant; $C_{1\text{-}5}$, fixed constants; and $T$, the absolute temperature. Much smaller induced polar forces are neglected from consideration here. The key indicator of whether segment–solvent interactions are favorable is the interchange energy of mixing $i$–$j$ pairs, $\omega$, given by

$$\omega = z[\Gamma_{ij} - \tfrac{1}{2}(\Gamma_{ii} + \Gamma_{jj})] \quad (2)$$

where $z$ is the number of dissimilar solvent–segment pairs. The choice of a suitable SCF solvent for a fractionation depends on the physical properties of the solvent that will intimately affect the interchange energy. However, since SCF solvents are highly compressible, it is important to be aware of how the quality of the solvent depends on its density. Lee[16] showed that the internal energy of a mixture, $u_{\text{total}}$, depends on the density of the solvent for a homogeneous-isotropic solution:

**Table I Structure and Physical Property Information for the Poly(ethylene-*co*-methyl acrylate) Copolymers Used in This Study**

| Comonomer Structure | |
|---|---|
| Ethylene<br>($\mu$ = 0.0 D $\alpha = 45 \cdot 10^{-25}$ cm$^3$)<br>—$H_2C$—$CH_2$— | Methyl Acrylate<br>($\mu$ = 1.7 D $\alpha = 88 \cdot 10^{-25}$ cm$^3$)<br>—$H_2C$—CH—<br>\|<br>C=O<br>\|<br>O<br>\|<br>$CH_3$ |

| Copolymer Properties | | | | | |
|---|---|---|---|---|---|
| Copolymer | Methyl Acrylate (wt %) | $M_w$ | $M_n$ | $M_w/M_n$ | Crystallinity (%) |
| $EMA_{70/30}$ | 29.9[c] | 123,800 | 36,400 | 3.4 | 20 |
| $EMA_{60/40}$ | 39.3[d] | 140,300 | 40,500 | 3.5 | 10 |
| $EMA_{40/60}$ | 63.2[d] | 108,900 | 33,000 | 3.3 | 0 |
| $EMA_{30/70}$ | 73.3[d] | 110,400 | 42,000 | 2.6 | 0 |

The copolymers are designated $EMA_{a/b}$, where a/b represents the weight percent of ethylene and methyl acrylate in backbone, respectively. The polarizability is $\alpha$ and the dipole moment, $\mu$, is in units of Debye (D).

[c] Determined by FTIR.

[d] Determined by NMR.

**Table II Physical Properties[17] of the Five Solvents Used to Fractionate Poly(ethylene-*co*-methyl acrylate Copolymers**

| Solvent | $T_C$ (°C) | $P_C$ (bar) | $\rho_C$ (g/mL) | $\alpha \cdot 10^{25}$ (cm$^3$) | $\mu$ (Debye) |
|---|---|---|---|---|---|
| Propane | 96.7 | 42.5 | 0.217 | 62.9 | 0 |
| Propylene | 91.9 | 46.2 | 0.236 | 62.6 | 0.4 |
| F22[a] | 96.2 | 49.7 | 0.522 | 61.5 | 1.5 |
| *n*-Butane | 152.1 | 38.0 | 0.228 | 81.4 | 0 |
| 1-Butene | 146.5 | 39.7 | 0.236 | 79.1 | 0.3 |

The polarizability is $\alpha$, [18] and the dipole moment is $\mu$.
[a] Chlorodifluoromethane.

$$\frac{u_{\text{total}}}{kT} \approx A_0 + A_1\rho \int u(r)g(r)\, r^2\, dr \qquad (3)$$

where $u(r)$ is the pair potential energy of *ii*, *jj*, and *ij* interactions; $g(r)$, the radial distribution function; $A_0$ and $A_1$, constants that depend on the properties of the components in solution; and $\rho$, the solvent density if the solution is moderately dilute in solute. This simplified formula provides an explanation for the "heuristic" that, to a first approximation, the solubility of a solute in an SCF solvent is proportional to density. This formula also shows why this heuristic is only true to a first approximation since a great amount of physics is buried in the $u(r)$ and $g(r)$ terms. Equations (1)–(3) provide some insight when choosing an appropriate SCF solvent for a given fractionation. It is important to match the physical properties of the SCF solvent with those of the solute so that the interchange energy is of sufficient strength to insure finite polymer solubilities at the conditions of the fractionation. However, it is also important that the interchange energy does not overwhelm the density effect so that the SCF solvent can be fine-tuned by manipulating its density with changes in the system temperature or pressure. Finally, eq. (1) shows that if temperature is varied the interchange energy can be adjusted through the $\Gamma_{ii}$ and $\Gamma_{jj}$ values to allow for increased solubilities of the polymer and to allow for an increased operating pressure range to fine-tune the solvent.

In this paper, we describe the fractionation of poly(ethylene-*co*-methyl acrylate) copolymers with respect to backbone composition as well as to molecular weight. Poly(ethylene-*co*-methyl acrylate) copolymers were chosen for this study since they are readily available with varying acrylate content and, therefore, the polar nature of the copolymer can be conveniently varied over a broad range. Table I lists the properties of the four poly(ethylene-*co*-methyl acrylate) copolymers (30, 40, 60, and 70 wt % methyl acrylate, $EMA_{30/70}$, $EMA_{40/60}$, $EMA_{60/40}$, and $EMA_{70/30}$, respectively) used in this study. As the acylate content is increased, the polarity of the copolymer increases substantially and the percent crystallinity decreases. Note also that the size and polarizability of a methyl acrylate repeat unit are much greater than that of an ethylene repeat unit. All the four copolymers have similar molecular weights and polydispersities. By judiciously choosing an SCF solvent, it is shown that either ethylene-

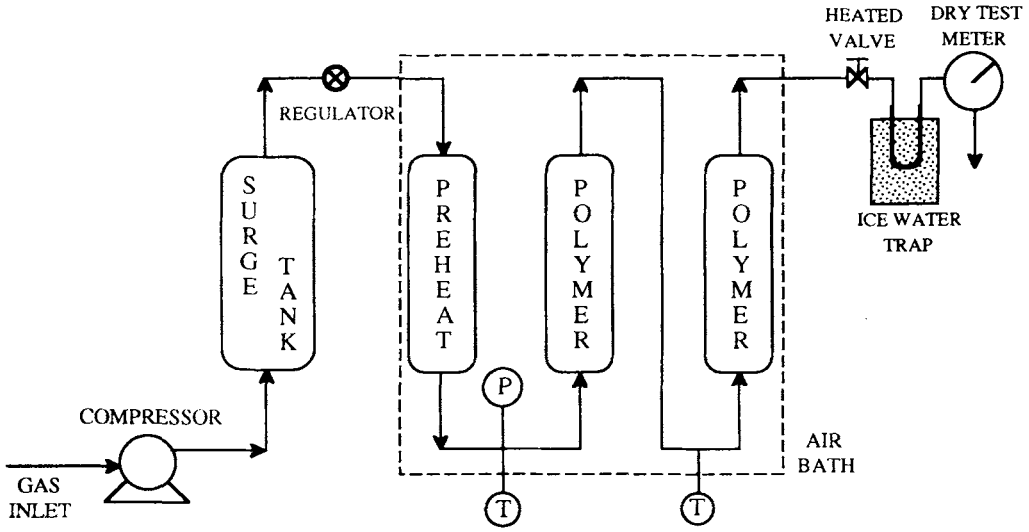


**Figure 1** Schematic diagram of the high-pressure flow apparatus used to fractionate polymers.

rich (nonpolar) or acrylate-rich (polar) oligomers can be selectively removed from the parent material. Table II lists the physical properties of the candidate SCF solvents used in this study. Propane, propylene, and chlorodifluoromethane (F22) have similar critical temperatures and pressures, but very different densities and polarities. Based on available literature information, nonpolar propane will be a good solvent for the high ethylene-content copolymers, whereas propylene will be a moderately good solvent for the acrylate-rich copolymers due to the favorable interaction of the dipole moment of the acrylate group in the copolymer with the double bond in propylene that gives it a quadrupole moment.[19,20] F22 is expected to be an excellent solvent for the high acrylate-content copolymers since F22 hydrogen bonds to methyl acrylate, but it does not hydrogen bond to itself.[10,19,21,22] Butane and butene, which have higher polarizabilities than those of the $C_3$ hydrocarbons, are used in this study since lower pressures should be needed to solubilize the high acrylate-content copolymers than those needed with the $C_3$ hydrocarbons. Therefore, it will be possible to perform fractionations with butane and butene without having to modify the existing experimental equipment to operate to higher pressures.

Cloud-point data are presented along with fractionation data to demonstrate how a rapid screening study can be used to facilitate the choice of fractionation solvent. Clearly, it is preferable to calculate the solubilities of the various copolymers in the candidate solvents; however, the state of the art for such calculations is not well developed for high-pressure, polymer–solvent mixtures that exhibit polar and

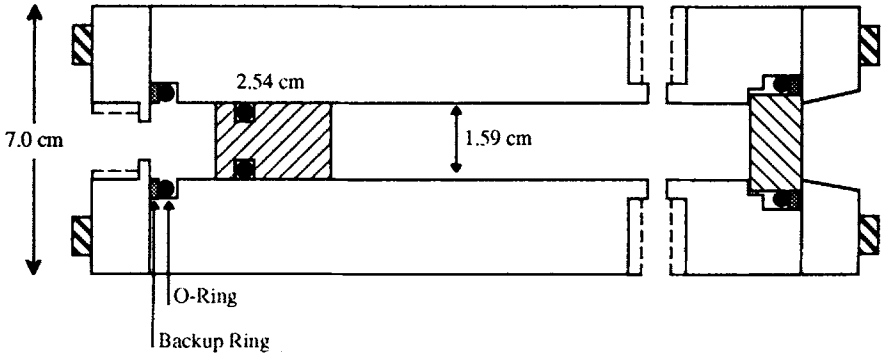


(A)

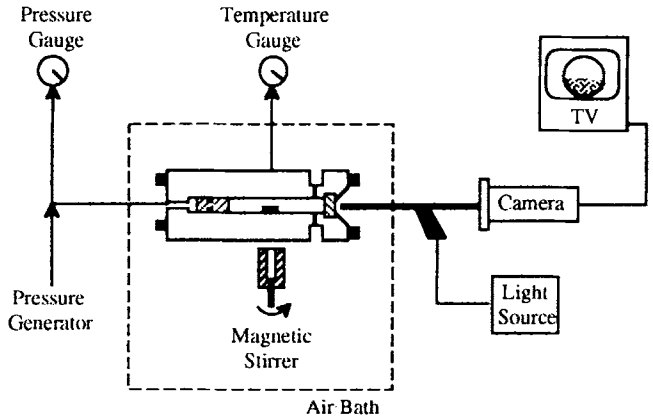


(B)

**Figure 2** Schematic diagram of the apparatus used to obtain cloud-point data: (A) schematic of the variable-volume, high-pressure view cell; (B) schematic of the entire apparatus.

hydrogen-bonding interactions. The cloud-point data needed to interpret the fractionation results not found in the literature will be obtained in this study. The following section briefly describes the experimental equipment and techniques used to obtain fractionation and cloud-point data.

## EXPERIMENTAL

The fractionation was performed using a dynamic flow apparatus capable of operating to 200°C and 650 bar (Fig. 1).[10] Glass wool was packed into the bottom of the first extraction column and into the top of the second column (1.8 cm i.d. × 30 cm long) and ~ 12 g of polymer was loaded into each column. SCF solvent was supplied to a diaphragm compressor (Superpressure, Model J46-14025-1), compressed, and delivered to a surge tank that was normally maintained at 690 bar. The SCF was then throttled through a pressure-reducing regulator (Tescom, Model 26-1000) and delivered to the columns at a flow rate in the range of 2.5–7.0 L/min (STP) (~ 6.0 g/min). The system pressure through the columns was controlled to within ±5.0 bar using the regulator, and the flow rate was controlled by manipulating the heated valve (HIP Inc, Model 30-12HF4-HT) at the outlet to the columns. Before entering the extraction columns, the SCF flowed through a preheater to reach thermal equilibrium with the air bath. The temperature of the gas was maintained to within ±1.0°C as measured with two platinum-resistance thermal devices located at the entrances of each extraction column.

The columns were first purged with nitrogen at room temperature to remove any air before introducing SCF solvent to the columns. The system was heated to the desired system temperature and allowed to equilibrate for 30 min under a blanket of SCF solvent. The column pressure was then fixed and the first sample was obtained. The loaded SCF exiting the column was expanded through a heated valve where polymer precipitated into a preweighed U-tube in an ice-water bath. Glass-wool filters at the exit of the U-tube trapped any fine mist entrained in the gas. The gas was routed to a dry-test meter (Singer American Meter Division, Model DTM-200) to monitor the total volume passed through the extractors. After about 55 min, the operating pressure was increased to the next desired pressure to obtain the next polymer fraction. The polymer samples in the U-tubes are weighed and analyzed for molecular weight and molecular weight distribution using gel-permeation chromatography with polystyrene standards, for crystallinity using DSC, and for acrylate content using $^{H}$NMR and FTIR.

Cloud-point curves are obtained using the apparatus shown in Figure 2 and described in detail elsewhere.[10,23] The high-pressure cell, constructed of a high nickel content steel (Nitronic 50, Armco Inc.), has a 1.59 cm i.d. and a 7.0 cm o.d., a working volume of ~ 35 cm$^3$, and is fitted with a 1.9 cm-thick sapphire window to view the phase behavior and with a moveable piston that is sealed with O-rings to adjust the system pressure. A known amount of polymer, to within ±0.002 g, is loaded into the cell, which is then purged at room temperature with the solvent at 3–6 bar to remove any entrapped air. The solvent of interest is then transferred into the

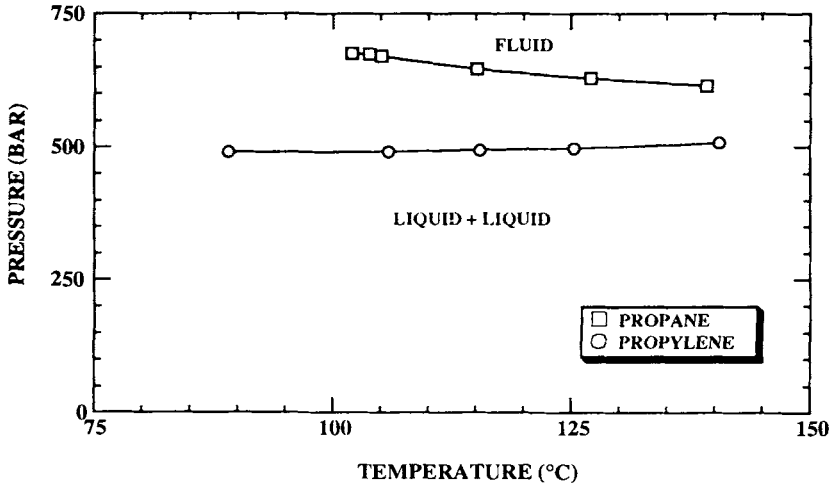


**Figure 3** Cloud-point curves for $EMA_{70/30}$ in propane and propylene obtained in this study.

cell gravimetrically to within ±0.002 g using a high-pressure bomb. The pressure of the polymer solution is determined by measuring the pressure (Heise gauge, accurate to within ±2.8 bar) of the fluid behind the piston. A small correction of ~ 1 bar is added to the pressure to account for the pressure needed to move the piston. The temperature of the cell is measured and maintained to within ±0.2°C using a platinum-resistance device connected to a digital multimeter. The contents of the cell are mixed by a stir bar activated by a magnet located below the cell. The polymer–SCF mixture in the cell is projected onto a video monitor using a borescope (Olympus Corporation, Model F100-024-000-55) placed against the sapphire window and connected to a video camera. The cloud-point pressure is defined as the point at which the mixture becomes so opaque that it is no longer possible to see the stir bar in the solution. The cloud-point curves are repeated at least twice at each temperature and are reproducible to within ±5 bar. Cloud-point determinations are done at constant polymer concentration, which in this study is maintained between 4.5 and 5.5 wt %.

## RESULTS

The fractionation and phase behavior data are presented in order of increasing polarity of the copolymer starting with $EMA_{70/30}$. The phase behavior of $EMA_{70/30}$ in propane and propylene is shown in Figure 3. The cloud-point curves in butane and butene are not shown since they are at such low pressures that it is not possible to effectively "fine-tune" these solvents during a fractionation. The cloud-point curve in chlorodifluoromethane is also not shown since the parent copolymer is not completely soluble in chlorodifluoromethane. However, this is not a negative finding because it suggests that chlorodifluoromethane should be used as the first solvent to remove only the acrylate-rich oligomers from the parent material. If either propane or propylene is used first, the entire parent copolymer could be fractionated since the cloud points are at pressures that are lower than the highest operating pressure of the equipment (~ 650 bar).

Fractionation data are shown in Table III for $EMA_{70/30}$ fractionated with chlorodifluoromethane followed by propane, both at 151°C. Chlorodifluoromethane is only able to extract ~ 68% of the copolymer charged to the fractionation columns. The polydispersities of the first seven fractions are about one-half that of the parent material even though sample sizes of 1–2 g are obtained at each pressure level. The concentration of methyl acrylate in the backbone of the copolymer is about 4 wt % greater than that in the parent material, confirming that chlorodifluoromethane preferentially solubilizes the more polar oligomers.

**Table III Data for the Fractionation of $EMA_{70/30}$ with Chlorodifluoromethane and Propylene at 151°C**

| No. | $P$ (bar) | Σ (wt %)[a] | Sample Wt (g) | $M_w$ | $M_w/M_n$ | MA[b] (wt %) |
|---|---|---|---|---|---|---|
| Chlorodifluoromethane | | | | | | |
| 1 | 308 | 4 | 0.58 | 10,500 | 1.5 | 32.5 |
| 2 | 375 | 12 | 1.09 | 18,300 | 1.3 | 33.5 |
| 3 | 449 | 28 | 2.11 | | | |
| 4 | 482 | 36 | 1.09 | 44,000 | 1.3 | 33.1 |
| 5 | 514 | 47 | 1.40 | 50,800 | 1.3 | 32.9 |
| 6 | 551 | 60 | 1.79 | 80,400 | 1.5 | 31.1 |
| 7 | 588 | 68 | 1.02 | | | 30.9 |
| Propane | | | | | | |
| 8 | 484 | 70 | 0.27 | | | 26.1 |
| 9 | 507 | 74 | 0.57 | | | 25.5 |
| 10 | 528 | 83 | 1.12 | 30,700 | 2.1 | 26.3 |
| 11 | 558 | 93 | 1.32 | 43,400 | 2.4 | 25.2 |
| 12 | 591 | 99 | 0.87 | 43,800 | 2.2 | 26.1 |
| 13 | 624 | 100 | 0.12 | 62,100 | 2.6 | 25.1 |
| Parent | | | 13.35 | 123,800 | 3.4 | 29.9 |

[a] Cumulative amount of copolymer removed from the columns.
[b] Methyl acrylate content as determined by FTIR.

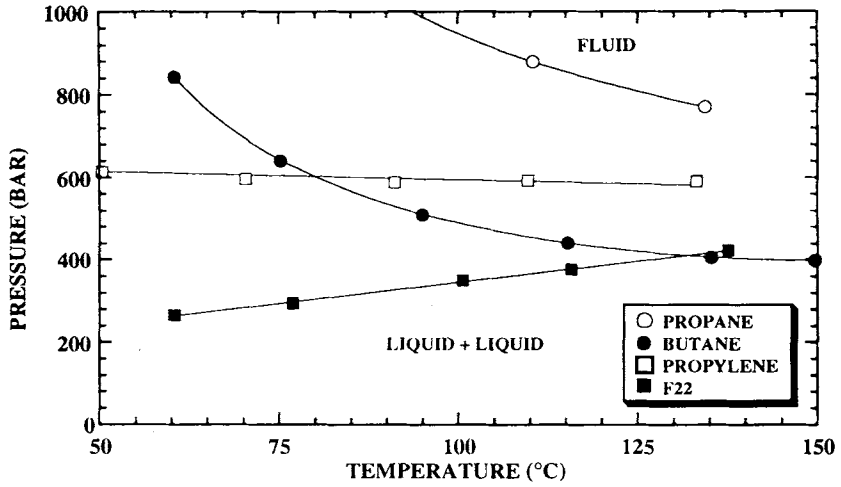


**Figure 4** Cloud-point curves for $EMA_{60/40}$ in propane,[20] propylene,[20] butane, and chlorodifluoromethane (F22). The cloud-point data in F22 and butane were obtained in this study.

Fractions 8–13 were obtained with propane. Again, the polydispersities of the fractions are less than that of the parent material. The concentration of methyl acrylate in the backbone of the fractions is now about 4 wt % less than that of the parent. Also, molecular weights of the first few fractions obtained with propane are lower than those of the final fractions obtained with chlorodifluoromethane, indicating that chlorodifluoromethane can only remove fractions that are rich in acrylate even if the molecular weight is greater than available oligomers that have a higher ethylene content.

The phase behavior of $EMA_{60/40}$ in propane, propylene, butane, and chlorodifluoromethane (F22) is shown in Figure 4. In this instance, both F22 and butane completely solubilize the parent copolymer at very low pressures. As a consequence, neither F22 nor butane should not be used first in the fractionation since each is too "good" a solvent. The phase behavior data suggest that propane should be used first to remove the ethylene-rich oligomers and that propylene, butane, or F22 could then be used to remove the rest of the parent material. Propane is not expected to fractionate the entire parent copolymer at temperatures below about 135°C since the pressures needed to obtain a single phase exceed the upper limit of the apparatus. Notice that propylene and F22 become less discriminatory as the temperature increases above about 135°C, where polar interactions between two acrylate segments in the copolymer and between a polar solvent molecule and an acrylate segment are expected to decrease, as shown in eq. (1). Hence, the cloud-point curves come closer together in pressure at high temperatures despite the large differences in polarity of the solvents as noted in Table II. It is interesting that the cloud-point curves in propane and propylene are significantly different from one another especially at low temperatures where polar forces are expected to be strongest. This difference is attributed to the slight dipole moment in propylene and to the quadrupole moment in propylene that is a result of the unsaturated double bond. Both of these polar moments enhance the interchange energy between a propylene segment and a segment of $EMA_{60/40}$.

Fractionation data are given in Table IV for $EMA_{60/40}$ fractionated with propane first and then with propylene at 130°C. Propane is only able to extract ~ 31% of the copolymer charged to the fractionation columns. The polydispersities of the first six fractions are less than that of the parent material and the concentration of methyl acrylate in the backbone of the fractions is only about 0.5 wt % less than that of the parent material.

Fractions 7–13 were obtained with propylene. Again, the polydispersities of the fractions are much less than that of the parent material. The concentration of methyl acrylate in the backbone of these fractions is about 3.6 wt % greater than that of the parent. Also, notice that the molecular weight of the first fraction obtained with propylene is lower than that of the final fraction obtained with propane, indicating that propane can only remove fractions that are lean in acrylate even if the molecular weight is greater than available oligomers that have a higher acrylate content.

**Table IV Data for the Fractionation of $EMA_{60/40}$ with Propane and Propylene at 130°C**

| No. | $P$ (bar) | $\Sigma$ (wt %)[a] | Sample Wt (g) | $M_w$ | $M_w/M_n$ | MA[b] (wt %) |
|---|---|---|---|---|---|---|
| Propane | | | | | | |
| 1 | 449 | 1 | 0.26 | 14,400 | 2.6 | 38.7 |
| 2 | 488 | 5 | 0.57 | 20,400 | 2.3 | 38.2 |
| 3 | 524 | 9 | 0.87 | 27,800 | 2.1 | 38.7 |
| 4 | 552 | 14 | 0.90 | 31,200 | 2.0 | 38.5 |
| 5 | 587 | 21 | 1.22 | 41,100 | 1.7 | |
| 6 | 624 | 31 | 1.86 | 52,800 | 1.5 | 39.7 |
| Propylene | | | | | | |
| 7 | 449 | 33 | 0.29 | 46,400 | 1.7 | 41.6 |
| 8 | 484 | 36 | 0.61 | 73,500 | 1.5 | 45.0 |
| 9 | 507 | 47 | 2.00 | 88,500 | 1.4 | |
| 10 | 528 | 60 | 2.23 | 127,800 | 1.7 | 42.9 |
| 11 | 558 | 80 | 3.70 | 202,900 | 1.8 | 42.7 |
| 12 | 591 | 91 | 1.89 | 334,300 | 2.1 | |
| 13 | 624 | 94 | 0.67 | | | 42.9 |
| Parent | | | 18.11 | 140,300 | 3.5 | 39.3 |

[a] Cumulative amount of copolymer removed from the columns.
[b] Methyl acrylate content as determined by NMR.

$EMA_{60/40}$ was also fractionated with F22 to confirm that chlorodifluoromethane is too "good" a solvent for this copolymer; the results are given in Table V. Using very small pressure increments, 14 fractions were obtained with modest polydispersities. No discernible trend was detected with the backbone composition of the fractions, indicating that F22 was only able to discriminate on the basis

**Table V Data for the Fractionation of $EMA_{60/40}$ with Chlorodifluoromethane at 150°C**

| No. | $P$ (bar) | $\Sigma$ (wt %)[a] | Sample Wt (g) | $M_w$ | $M_w/M_n$ | MA[b] (wt %) |
|---|---|---|---|---|---|---|
| 1 | 137 | 1 | 0.15 | 1,100 | 1.4 | |
| 2 | 171 | 2 | 0.15 | 3,300 | 1.7 | |
| 3 | 205 | 4 | 0.28 | 5,900 | 1.5 | |
| 4 | 241 | 7 | 0.34 | 7,800 | 1.5 | |
| 5 | 274 | 10 | 0.50 | 10,000 | 1.7 | |
| 6 | 309 | 17 | 0.90 | 26,500 | 1.5 | 45.3 |
| 7 | 330 | 28 | 1.48 | 32,400 | 1.5 | 40.4 |
| 8 | 343 | 36 | 1.11 | 47,100 | 1.5 | 40.4 |
| 9 | 364 | 46 | 1.33 | 58,200 | 1.4 | 42.7 |
| 10 | 385 | 58 | 1.55 | 78,100 | 1.5 | 44.1 |
| 11 | 406 | 75 | 2.31 | 105,600 | 1.5 | 40.8 |
| 12 | 424 | 83 | 1.11 | 162,500 | 2.5 | 41.1 |
| 13 | 446 | 94 | 1.45 | 239,100 | 1.7 | 42.3 |
| 14 | 470 | 100 | 0.87 | 513,700 | 1.5 | 43.4 |
| Parent | | | 13.53 | 140,300 | 3.5 | 42.4 |

[a] Cumulative amount of copolymer removed from the columns.
[b] Methyl acrylate content as determined by FTIR.

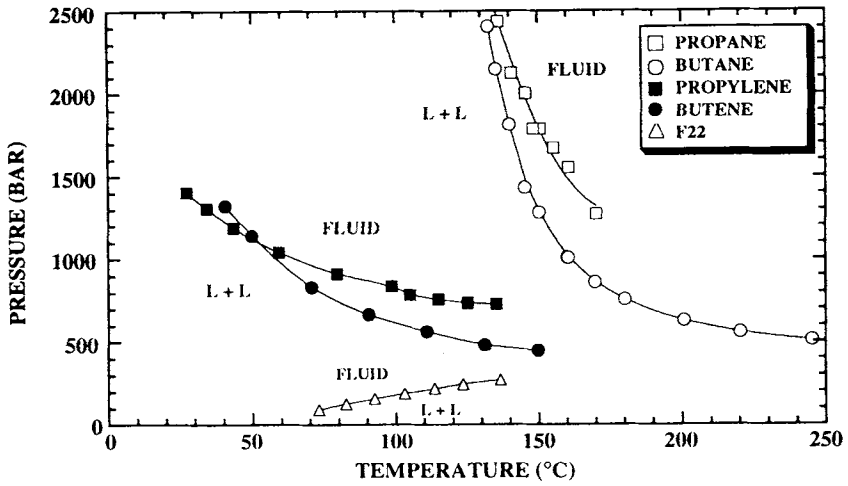


**Figure 5** Cloud-point curves for $EMA_{40/60}$ in propane,[20] butane, propylene,[20] 1-butene, and chlorodifluoromethane (F22).[10] The cloud-point data in butane and butene were obtained in this study.

of molecular weight and not on the basis of composition. The fractionation and cloud-point data both highlight the impact of hydrogen bonding on the fractionation behavior. Although it was possible to decrease the solvent strength of propane by operating at a modest temperature to fractionate with respect to copolymer chemical composition, this was not possible with F22, presumably because hydrogen bonding between the solvent and the acrylate groups was too strong even at 150°C. F22 is indeed a high-quality solvent for this copolymer even at modest pressures of less than 500 bar. This is in contrast to the previous case where F22 was not capable of dissolving the parent material that had only 10 wt % fewer acrylate groups.

The phase behavior of $EMA_{40/60}$ in propane, butane, propylene, 1-butene, and chlorodifluoromethane (F22) is shown in Figure 5. The pressure and temperature axes are expanded in this instance since the cloud-point data for $EMA_{40/60}$ in butane and 1-butene are original data obtained in this study. The propane cloud-point curve is shifted to slightly higher temperatures than is the butane curve because of the meager solvent power of propane. The cloud-point curves in both of the saturated hydrocarbons rise very steeply in pressure for small changes in temperature in the range of 130–175°C. Evidently, the polar polymer–polymer interactions are highly favored as the temperature decreases, as suggested in eq. (1). The cloud-point curves in the unsaturated hydrocarbons increase in pressure with decreasing temperature much less radically. Also, the impact of hydrogen bonding is evident with the F22 cloud-point curve, which is located at very low pressures. It is impractical to use propane to fractionate $EMA_{40/60}$ since the pressures needed to obtain a single phase are more than 1000 bar greater than the highest operating pressure obtainable with the fractionation equipment. The two solvents chosen for fractionating $EMA_{40/60}$ are butane at 139°C and 1-butene at 118°C. Although both operating temperatures are below the critical temperature of the respective solvents, a good fractionation can be obtained since these two "near-critical" solvents are highly compressible. Also, in the temperature range of 115–140°C, the respective cloud-point curves are at very different pressures, suggesting that it may be possible to remove the ethylene-rich oligomers with butane and the acrylate-rich oligomers with butene.

Fractionation data are shown in Table VI for $EMA_{40/60}$ fractionated with butane first and then with 1-butene. Butane extracts ~ 21% of the copolymer charged to the columns. The polydispersities of the first six fractions are less than one-half that of the parent material, although the concentration of methyl acrylate in the backbone of the copolymer for these fractions is essentially the same as that of the parent material.

Fractions 7–14 were obtained with 1-butene at 118°C, a subcritical temperature. Again, the polydispersities of the fractions are much less than that of the parent material and the concentration of methyl acrylate in the backbone of the copolymer is essentially the same as that of the parent material. Also, notice that molecular weight of fraction 7 ob-

**Table VI Data for the Fractionation of $EMA_{40/60}$ with Butane and 1-Butene at Subcritical Temperatures**

| No. | $P$ (bar) | $\Sigma$ (wt %)[a] | Sample Wt (g) | $M_w$ | $M_w/M_n$ | MA[b] (wt %) |
|---|---|---|---|---|---|---|
| Butane at 139°C | | | | | | |
| 1 | 382 | 4 | 0.79 | 19,600 | 1.4 | 61.7 |
| 2 | 414 | 6 | 0.52 | 22,600 | 1.3 | 63.4 |
| 3 | 448 | 9 | 0.56 | 28,600 | 1.4 | 62.4 |
| 4 | 500 | 13 | 0.87 | 35,500 | 1.3 | 61.9 |
| 5 | 561 | 16 | 0.43 | 54,500 | 1.6 | 61.4 |
| 6 | 637 | 21 | 1.07 | 51,000 | 1.3 | 62.5 |
| 1-Butene at 118°C | | | | | | |
| 7 | 276 | 24 | 0.74 | 53,000 | 1.2 | 62.0 |
| 8 | 310 | 31 | 1.38 | 68,900 | 1.4 | 61.9 |
| 9 | 337 | 40 | 1.86 | 68,800 | 1.2 | 62.0 |
| 10 | 368 | 50 | 2.09 | 87,300 | 1.2 | 61.8 |
| 11 | 396 | 66 | 3.16 | 112,100 | 1.2 | 61.9 |
| 12 | 430 | 81 | 3.07 | 152,700 | 1.2 | 61.7 |
| 13 | 465 | 91 | 1.97 | 178,200 | 1.2 | |
| 14 | 521 | 100 | 1.92 | 277,900 | 1.3 | |
| Parent | | | 20.44 | 108,900 | 3.3 | 63.2 |

[a] Cumulative amount of copolymer removed from the columns.
[b] Methyl acrylate content as determined by NMR.

tained with 1-butene is slightly greater than the final fraction obtained with butane, indicating that butane does not discriminate by chemical composition. This lack of chemical discrimination was somewhat surprising since the shape and location of the butane cloud point curve in P–T space suggests that highly polar EMA oligomers should not readily be dissolved at 139°C. One plausible explanation for the poor fractionation with respect to chemical composition is that the parent $EMA_{40/60}$ has a narrow chemical composition distribution and it is not possible to fractionate it any further. Based on the results reported here for $EMA_{60/40}$, the chemical composition distribution for $EMA_{40/60}$ need only be less than about ±2 wt %.

The phase behavior of $EMA_{30/70}$ in propylene, 1-butene, butane, and chlorodifluoromethane (F22) is shown in Figure 6. At low temperatures, the cloud-point curve for butene is at higher pressures than that for propylene, whereas at higher temperatures, the opposite behavior is observed. This shift in the two cloud-point curves is probably a consequence of the smaller quadrupole per unit volume in butene, making it a less effective solvent at low temperatures even though it has a higher polarizability than that of propylene. At higher temperatures where polar interactions are expected to be diminished [see eq. (1)], the butene curve is now at pressures below that of the propylene curve. The cloud-point curve for F22, an excellent solvent for $EMA_{30/70}$, is at very low pressures, making it an unattractive fractionation solvent in this instance. The enhanced solvent power of F22 relative to butene, the physically larger solvent, is attributed to the hydrogen bonding between F22 and $EMA_{30/70}$. For this fractionation, propylene will be used first, followed by butene.

Table VII shows the results for $EMA_{30/70}$ fractionated with propylene at 137°C and then with 1-butene at 157°C. Propylene, to a pressure of 650 bar, is only able to extract ~ 11% of the copolymer charged to the columns. The polydispersities of the first six fractions are quite modest, although the concentration of methyl acrylate in the backbone of the copolymer for these fractions is essentially the same as that of the parent material. Evidently, the high acrylate content of this copolymer makes the high molecular weight oligomers essentially insoluble in propylene at pressures to ~ 650 bar. This solubility behavior is not entirely unexpected, since the cloud-point pressure of $EMA_{30/70}$ in propylene at this temperature is greater than the operating pressure of the fractionation apparatus.

Fractions 7–18, obtained with 1-butene, have small polydispersities and essentially the same concentration of methyl acrylate in the backbone of the copolymer as that of the parent material. It may

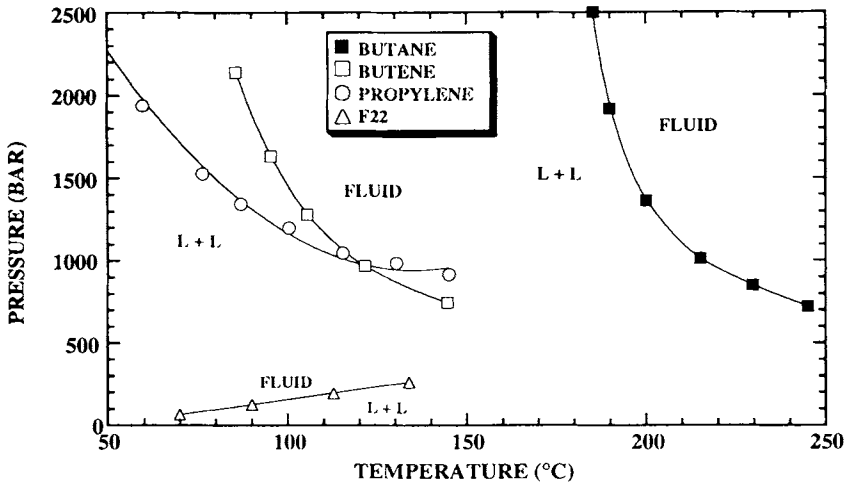


**Figure 6** Cloud-point curves for $EMA_{30/70}$ in propylene,[20] 1-butene, butane, and chlorodifluoromethane (F22). The cloud-point data in F22, butene, and butane were obtained in this study.

also be that the parent $EMA_{30/70}$ has a chemical composition distribution that is less than about ±2 wt %, and it is not possible to fractionate it any further.

To test the efficacy of fractionating with respect to chemical composition, the four copolymers were combined in the proportions given in Table VIII to produce an artificial mixture of 44 wt % ethylene

**Table VII Data for the Fractionation of $EMA_{30/70}$ with Propylene at 137°C and with 1-Butene at 157°C**

| No. | $P$ (bar) | Σ (wt %)[a] | Sample Wt (g) | $M_w$ | $M_w/M_n$ | MA[b] (wt %) |
|---|---|---|---|---|---|---|
| Propylene at 137°C | | | | | | |
| 1 | 482 | 2 | 0.34 | 9,600 | 2.3 | |
| 2 | 518 | 3 | 0.37 | 11,600 | 1.7 | 71.7 |
| 3 | 553 | 5 | 0.36 | 15,300 | 1.7 | 71.8 |
| 4 | 588 | 7 | 0.42 | 18,500 | 1.5 | |
| 5 | 622 | 9 | 0.40 | 21,900 | 1.4 | |
| 6 | 656 | 11 | 0.60 | 26,200 | 1.3 | |
| 1-Butene at 157°C | | | | | | |
| 7 | 244 | 15 | 0.84 | | | |
| 8 | 277 | 16 | 0.14 | | | |
| 9 | 344 | 18 | 0.46 | 38,900 | 1.5 | |
| 10 | 415 | 26 | 1.84 | 46,300 | 1.4 | 73.9 |
| 11 | 450 | 34 | 1.60 | 55,300 | 1.3 | |
| 12 | 485 | 48 | 3.16 | 68,100 | 1.3 | 73.3 |
| 13 | 506 | 59 | 2.36 | 82,900 | 1.3 | |
| 14 | 527 | 66 | 1.60 | 102,500 | 1.3 | 72.3 |
| 15 | 548 | 73 | 1.63 | 114,100 | 1.3 | |
| 16 | 579 | 84 | 2.36 | 142,400 | 1.3 | 72.0 |
| 17 | 621 | 96 | 2.54 | 173,900 | 1.3 | |
| 18 | 653 | 100 | 0.96 | 247,400 | 1.3 | |
| Parent | | | 21.92 | 110,400 | 2.6 | 73.3 |

[a] Cumulative amount of copolymer removed from the columns.
[b] Methyl acrylate content as determined by NMR.

**Table VIII Proportions of the Four Copolymers Used to Make $EMA_{44/56}$**

| Parent Polymer | Weight (g) |
|---|---|
| $EMA_{70/30}$ | 1.03 |
| $EMA_{60/40}$ | 9.06 |
| $EMA_{40/60}$ | 6.92 |
| $EMA_{30/70}$ | 6.87 |

and 56 wt % methyl acrylate ($EMA_{44/56}$) that was fractionated, in order, with propane at 132°C, butane at 147°C, propylene at 147°C, and 1-butene at 157°C. The properties of the parent mixture are given in the last line of Table IX. Note that there are three glass transition temperatures ($T_g$) listed, which represent the $T_g$'s of $EMA_{60/40}$, $EMA_{40/60}$, and $EMA_{30/70}$. The $T_g$ for $EMA_{70/30}$ is not observed in the DSC scan of the parent mixture, probably because it is masked by the transition of $EMA_{60/40}$. The results of this fractionation are shown in Table IX. The first five fractions obtained with propane have polydispersities that are much less than that of the starting material. Based on a mass balance, the DSC analysis, and the chemical composition analysis, propane has extracted most of $EMA_{70/30}$ and about half of the available $EMA_{60/40}$.

The analyses of fractions 6–13 suggest that butane has removed the rest of $EMA_{60/40}$ and about 2 g of $EMA_{40/60}$ from the starting material. It is interesting that fractions 7, 8, and 9 are each more than twice as large as fractions 10, 11, 12, and 13, even though the pressure has increased steadily for each fraction and, therefore, the solvent power of butane also increased for each fraction. The explanation for the decrease in sample size with increasing solvent power is apparent from the trends in the chromatograms of fractions 6–13 given in Figure 7. The chromatograms of fractions 6, 7, and 8 show an

**Table IX Data for the Fractionation of $EMA_{44/56}$**

| No. | $P$ (bar) | Σ (wt %) | Sample Wt (g) | $M_n$ | $M_w/M_n$ | MA[b] (wt %) | $T_{g1}$ (°C) | $T_{g2}$ (°C) | $T_{g3}$ (°C) | $T_{g4}$ (°C) | Crystallinity (%) |
|---|---|---|---|---|---|---|---|---|---|---|---|
| Propane at 132°C | | | | | | | | | | | |
| 1 | 408 | 2 | 0.44 | 12,200 | 1.7 | 40.7 | | | | | |
| 2 | 475 | 5 | 0.73 | 17,800 | 1.7 | 41.9 | −38.8 | | | | 8.8 |
| 3 | 548 | 9 | 1.09 | 20,600 | 2.2 | 42.5 | −36.6 | −31.0 | | | 11.2 |
| 4 | 606 | 15 | 1.27 | 37,600 | 2.2 | | −34.5 | −30.2 | | | 11.8 |
| 5 | 659 | 22 | 1.71 | 50,100 | 2.9 | 40.6 | | −33.9 | | | 11.2 |
| Butane at 147°C | | | | | | | | | | | |
| 6 | 323 | 25 | 0.77 | 60,500 | 2.5 | 44.7 | | −34.1 | | | 8.7 |
| 7 | 379 | 32 | 1.72 | 113,300 | 3.3 | 42.1 | | −32.6 | | | 9.2 |
| 8 | 416 | 39 | 1.70 | 172,000 | 4.1 | 43.4 | | −32.4 | | | 8.2 |
| 9 | 452 | 44 | 1.09 | 76,700[b] | 4.9 | 44.4 | | −31.0 | −26.7 | | 6.7 |
| 10 | 481 | 46 | 0.56 | 53,500[b] | 4.9 | 49.8 | | −30.9 | −25.9 | | 5.9 |
| 11 | 535 | 48 | 0.43 | 47,100[b] | 6.7 | 53.1 | | | −27.3 | | 5.2 |
| 12 | 491 | 49 | 0.34 | 37,800 | 3.8 | | | | −27.6 | | 2.9 |
| 13 | 660 | 51 | 0.44 | 42,012 | 2.2 | | | | −27.4 | | 1.7 |
| Propylene at 147°C | | | | | | | | | | | |
| 14 | 652 | 61 | 2.28 | 39,900 | 2.0 | 68.9 | | | −26.8 | −19.6 | 0.6 |
| 1-Butene at 157°C | | | | | | | | | | | |
| 15 | 346 | 63 | 0.51 | 66,400 | 1.6 | | | | −31.1 | −22.4 | 0.1 |
| 16 | 396 | 69 | 1.50 | 83,200 | 1.8 | 66.3 | | | −27.5 | −19.6 | 0.5 |
| 17 | 438 | 79 | 2.39 | 103,000 | 2.7 | 65.2 | | | −27.1 | −18.3 | 0.0 |
| 18 | 465 | 83 | 0.92 | 116,500[b] | 2.8 | | | | −25.3 | −15.8 | 0.0 |
| 19 | 523 | 87 | 0.93 | 93,900 | 1.6 | 72.3 | | | | −19.7 | 0.0 |
| 20 | 589 | 93 | 1.39 | 127,800 | 1.5 | 71.8 | | | | −18.1 | 0.0 |
| 21 | 652 | 100 | 1.69 | 201,200 | 1.8 | 69.5 | | | | −16.6 | 0.5 |
| Parent | | | 23.96 | 58,200 | 4.0 | 57.6 | | −33.8 | −26.8 | −18.1 | |

[a] As determined by FTIR.
[b] Bimodal chromatogram.

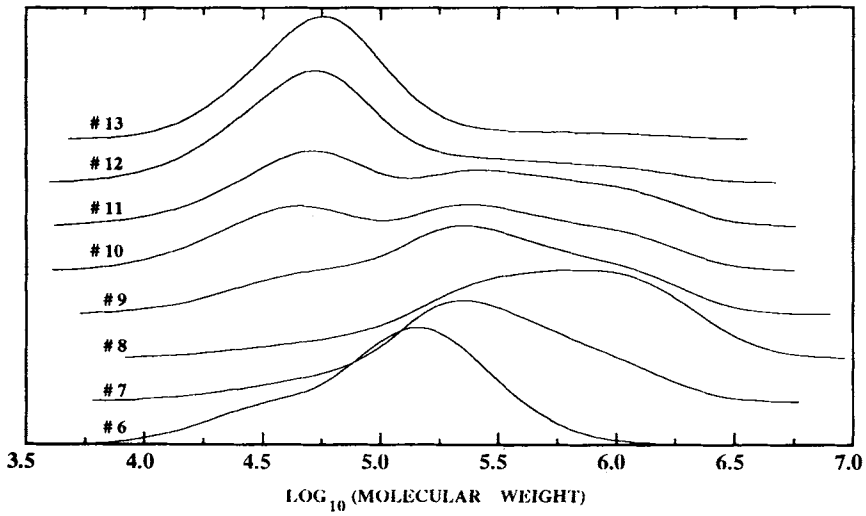


**Figure 7** Chromatograms for fractions 6–13 of $EMA_{44/56}$ given in Table IX.

increase in the molecular weight, as would be expected as the pressure increases. Also, the compositional analysis of these fractions shows that they are mostly composed of $EMA_{60/40}$ plus the $EMA_{70/30}$ that was left in the columns. However, the chromatogram for fraction 9 shows the beginning of a bimodal distribution of low molecular weight material with higher molecular weight material. This trend of mixing low and high molecular weight material in a single fraction is evident in the chromatograms of fractions 10 and 11. Also, the DSC scans of these three fractions reveal two $T_g$'s, suggesting that these fractions are blends of two EMA copolymers. The compositional analysis of fractions 10 and 11 show that these fractions are composed of a mixture of $EMA_{60/40}$ with some $EMA_{40/60}$. Finally, as the pressure is further increased for fractions 12 and 13, the bimodal character of the chromatograms and the occurrence of two $T_g$'s are eliminated as all of the $EMA_{60/40}$ is flushed from the columns, and the peak molecular weight also increases slightly with increasing pressure.

Note that even though propylene extracts 2.28 g of oligomers that are rich in $EMA_{40/60}$ the molecular weight distribution is much less than that of the starting material, probably because all of the $EMA_{70/30}$ and $EMA_{60/40}$ have been removed from the columns and because propylene has little affinity for $EMA_{30/70}$. At this point, there should be approximately 2.4 g of $EMA_{40/60}$ left in the columns.

With butene, we see many of the same trends that were observed with butane. The molecular weight of the fractions obtained with butene increase up to fraction 18, decrease for fraction 19, and then increase again with increasing pressure. Notice also that the composition of fractions 15–17 are lower in methyl acrylate than are fractions 19–21. More than likely, $EMA_{40/60}$ has been extracted from the columns with fractions 15–18, leaving only $EMA_{30/70}$ to be fractionated. The GPC chromatogram of fraction 18 reveals a small shoulder on the low molecular weight side of the GPC trace that is more than likely $EMA_{30/70}$. The DSC scans for fractions 15–18 also reveal two $T_g$'s, suggesting that these fractions are actually composed of $EMA_{40/60}$ and $EMA_{30/70}$. The analysis of the fractions obtained with butene shows conclusively that butene first dissolves the oligomers with the lower acrylate content even if the molecular weights of these oligomers are higher than those with the higher acrylate content. The reason that the polydispersities of fractions 15–21 are much lower than those for fractions 7–13 is that there are no low acrylate-content or low molecular weight oligomers available to be removed at the end of the fractionation.

## CONCLUSIONS

Supercritical fluid solvent fractionation is a rapid technique that provides gram-sized fractions of narrow molecular weight distribution. It is also possible to fractionate polymers with respect to their chemical composition using, in series, two or more SCF solvents of varying physical properties. The fractionation behavior with a given SCF solvent at given operating conditions is intimately linked with the P–T location of the polymer–SCF solvent cloud-

point curve. The principles of molecular thermodynamics can be used to qualitatively interpret the fractionation results and to provide insight into choosing a suitable SCF solvent and operating conditions for a particular fractionation.

The authors acknowledge the National Science Foundation for partial support of this project under grant CTS-9122003, and they acknowledge Bruce M. Hasch for helpful technical discussions concerning this paper.

## REFERENCES

1. V. J. Krukonis, *Polym. News,* **11,** 7 (1985).
2. S. V. Dhalewadikar, M. A. McHugh, and T. L. Guckes, *J. Appl. Polym. Sci.,* **33,** 521 (1987).
3. K. M. Scholsky, K. M. O'Connor, C. S. Weiss, and V. J. Krukonis, *J. Appl. Polym. Sci.,* **33,** 2925 (1987).
4. C. S. Elsbernd, D. K. Mohanty, J. E. McGrath, P. M. Gallagher, and V. J. Krukonis, *Polym. Prepr.,* **28,** 399 (1987).
5. M. A. McHugh and V. J. Krukonis, in *Encycl. Polym. Sci. Eng.,* 2nd Ed., vol. 16, John Wiley & Sons, Inc., New York, 1989, p. 368.
6. M. A. McHugh and V. J. Krukonis, *Supercritical Fluid Extraction: Principles and Practice,* 2nd ed., Butterworths, Boston, MA, to appear.
7. S. K. Kumar, S. P. Chhabria, R. C. Reid, and U. W. Suter, *Macromolecules,* **20,** 2550 (1987).
8. S. Krishnamurthy and S. H. Chen, *Makromol. Chem.,* **190,** 1407 (1989).
9. J. M. DeSimone, A. M. Hellstern, E. J. Siochi, S. D. Smith, T. C. Ward, P. M. Gallagher, V. J. Krukonis, and J. E. McGrath, *Makromol. Chem. Macromol. Symp.,* **32,** 21 (1990).
10. M. A. Meilchen, B. M. Hasch, and M. A. McHugh, *Macromolecules,* **24,** 4874 (1991).
11. J. J. Watkins and V. J. Krukonis, in *Proceedings of the 2nd International Symposium on Supercritical Fluids,* Boston, MA, 1991, pp. 37–41.
12. J. J. Watkins, V. J. Krukonis, P. D. Condo, D. Pradhan, and P. Ehrlich, *J. Supercritical Fluids,* **4,** 24 (1991).
13. C. A. Eckert, M. P. Ekart, B. L. Knutson, K. P. Payne, C. L. Tomasko, C. L. Liotta, and N. R. Foster, *Ind. Eng. Chem. Res.,* **31,** 1105 (1992).
14. W. M. Saltzman, N. F. Sheppard, M. A. McHugh, R. B. Dause, J. A. Pratt, and A. M. Dodrill, *J. Appl. Polym. Sci.,* to appear.
15. J. M. Prausnitz, R. N. Lichtenthaler, and E. G. Azevedo, *Molecular Thermodynamics of Fluid Phase Equilibria,* 2nd ed., Prentice-Hall, Englewood Cliffs, NJ, 1986.
16. L. L. Lee, *Molecular Thermodynamics of Nonideal Fluids,* Butterworths, Boston, MA, 1988.
17. R. C. Reid, J. M. Prausnitz, and B. E. Poling, *The Properties of Gases and Liquids,* 4th ed., McGraw-Hill, New York, 1987.
18. K. J. Miller and J. A. Savchik, *J. Am. Chem. Soc.,* **101,** 7206 (1979).
19. B. M. Hasch, M. A. Meilchen, S.-H. Lee, and M. A. McHugh, *J. Polym. Sci. Polym. Phys. Ed.,* to appear.
20. B. M. Hasch, M. A. Meilchen, S.-H. Lee, and M. A. McHugh, *J. Polym. Sci. Polym. Phys. Ed.,* **30,** 1365 (1991).
21. R. M. Izatt, R. S. Schofield, P. W. Faux, P. R. Harding, S. P. Christensen, and J. J. Christensen, *Thermochim. Acta,* **68,** 223 (1983).
22. M. Uematsu and E. U. Franck, *Ber. Bunsenges. Phys. Chem.,* **93,** 177 (1989).
23. M. A. Meilchen, B. M. Hasch, S.-H. Lee, and M. A. McHugh, *Polymer,* **33,** 1922 (1992).

*Received September 15, 1992*
*Accepted November 13, 1992*